Combining Monte Carlo and worst-case methods for trajectory prediction in air traffic control: A case study

E. Crisostomi
Department of Electrical Systems and Automation, University of Pisa, Italy
emanuele.crisostomi@gmail.com

A. Lecchini-Visintini
Department of Engineering, University of Leicester, UK
alv1@leicester.ac.uk

J. Maciejowski
Department of Engineering, University of Cambridge, UK
jmm@eng.cam.ac.uk

Abstract

We illustrate, through a case study, a novel combination of probabilistic Monte Carlo methods and deterministic worst-case methods to perform model-based trajectory prediction in Air Traffic Control. The objective is that of computing and updating predictions of the trajectory of an aircraft on the basis of received observations. We assume that uncertainty in computing the predictions derives from observation errors, from the action of future winds and from inexact knowledge of the mass of the aircraft. Our novel approach provides worst-case prediction sets to which the future trajectory of the aircraft is guaranteed to belong and, at the same time, an empirical distribution of the most probable trajectories which can be used to compute various estimates such as the probability of conflict and the expected time of arrival. The case study is developed using the aircraft performance model developed by the EUROCONTROL Experimental Centre in BADA (Base of Aircraft DAta).

Keywords: trajectory prediction, Air Traffic Control, worst-case methods, set-membership, Monte Carlo methods, particle filter, non-linear systems.

I. Introduction

The ability to compute a reliable prediction of the trajectory of an aircraft on a future horizon of the order of tens of minutes is an essential part of Air Traffic Control (ATC). Increasing levels of traffic both in Europe and in the US demand more advanced trajectory prediction algorithms in order to sustain the performance of ATC - see e.g. Paglione et al. [1].

A trajectory prediction is calculated on the basis of the aircraft estimated position and state, some intent information, weather information and a performance model. The aircraft position and state can be estimated from radar measurements or can be broadcast by the aircraft itself, such as in the Mode-S [2] and ADS-B [3] systems. The intent information includes controller instructions and operational procedures (e.g. how a descent is executed). The weather information includes predicted winds and temperature profiles. The performance model describes the aircraft dynamic behavior. Commercial aircraft in level flight can be modeled adequately by simple kinematic models - see e.g. Innocenti et al.[4], Frazzoli et al.[5], Paielli[6], and Mao et al.[7]. More complex performance models are needed only to calculate trajectories which include a change of altitude.

In a prediction on a future horizon of the order of tens of minutes there is unavoidable uncertainty. In the seminal papers of Paielli and Erzberger[8], [9], on the use of trajectory prediction to assess the probability of a future loss of safe separation between two aircraft (conflict probability), the approach for taking uncertainty into account is to superimpose a distribution of position errors on a predicted nominal trajectory. The distribution of position errors is estimated on the basis of previous radar track records - see also Yang and Kuchar[10]. In Yang et al.[11], the use of Monte Carlo methods for estimating conflict probability is proposed. In a model based approach, the predictions and their uncertainty are derived from models of the aircraft motion and its environment. In Chaloulos and Lygeros[12] a study is presented of the effect of spatial correlation of the winds on conflict probability based on Monte Carlo simulations of a sophisticated wind model. The problem of estimating the probability of future conflicts and mid-air collisions has been an important benchmark for the development of advanced speed-up techniques for Monte Carlo methods - see e.g. Blom et al.[13]. Worst-case assumptions have been adopted for example in Tomlin et al.[14] for the purpose of designing safe maneuvers to resolve the encounter of a set of aircraft in level flight.

In this paper we present a case study to illustrate a novel combination of Monte Carlo and worst-case methods to perform trajectory prediction. The case study is focused on a leg of flight which is typical of an aircraft descent in a Terminal Maneuvering Area (TMA) sector. The unknowns, in calculating the prediction from the point of view of ATC, are the mass of the aircraft and the action of the winds, which are realistic uncertainties in ATC[15], [16]. In our case study, we illustrate the advantages of using an aircraft performance model to calculate worst-case and probabilistic predictions at the same time. Here we adopt the aircraft performance model developed by the EUROCONTROL Experimental Centre in BADA (Base of Aircraft DAta)[17]. The use of the BADA[17] performance model does not pose any particular difficulty in the implementation of the Monte Carlo approach. On the other hand, it does entail the development of tailored algorithms for the implementation of the worst-case approach.

The paper is organized as follows. In the next section we review the Monte Carlo and worst-case approaches to estimation and prediction and present the idea of combining the two approaches. In *The case study* we describe the design of the case study, including the objective, the assumptions on the intent and the wind, and the adopted performance model. In *Worst-case prediction algorithms* we derive the algorithms for implementing the worst-case approach in our case study. In the following section, *Combining the Monte Carlo and worst-case approaches*, we present the novel algorithm which combines the Monte Carlo and worst-case approaches. In *Simulation examples* we provide an illustration of our algorithm using simulated scenarios of the proposed case study. In the last section we state our findings and conclude the paper.

Quantities are expressed in SI units throughout the paper. In some cases, lengths and altitudes are expressed also in feet (*ft*) and nautical miles (*nmi*) because these units are commonly employed in ATC.

II. The methods

In the stochastic Monte Carlo approach an empirical distribution of trajectory predictions is constructed by drawing random samples of the initial state and of the unknowns (in our case the mass of the aircraft and the wind) from Bayesian prior distributions and by running simulations of the aircraft performance model. Such an empirical distribution approximates the *a posteriori* distribution of the future trajectory given the priors on the unknowns and given the observations and the likelihood of observation errors. The sampled trajectory predictions obtained in this approach can be used to compute various estimates such as the probability of conflict with another aircraft and the expected time of arrival. The Monte Carlo approach extends the applicability of the popular Kalman filtering techniques to general non-Gaussian and non-linear models. On-line applications, such as trajectory prediction, require a computationally efficient implementation usually denoted *sequential Monte Carlo* or *particle filtering* - see e.g. Blom et al.[13], Gordon et al.[18], Van der Merwe et al.[19], Doucet et al.[20], Arulampalam et al.[21], and Künsch [22]. In particle filtering, the predictions are updated sequentially on the basis of the last received observation without the need to reprocess older observations each time a new observation is received. The appeal of a Monte Carlo approach stems from the fact that it can be used in very complex problems and, in general, is straightforward to implement since it simply requires simulations of the model to be run.

In the worst-case approach the aim is to compute guaranteed predictions in the form of sets containing all the trajectories which are consistent with the datum that the observation errors, the initial state and the unknowns belong to some given bounded uncertainty sets. In the context of estimation and filtering for dynamical systems this methodology is also referred to as the *set-membership* approach - see e.g. Schweppe [23], Bertsekas and Rhodes [24], Chisci et al.[25], and Polyak et al. [26]. In the set-membership approach the prediction set is updated recursively. The initial predictions are only consistent with the given uncertainty sets of the initial state and of the unknowns, which are defined by existing knowledge of the model. In our case, the mass of the aircraft is known to be confined between a known minimum and a known maximum and it can be assumed that errors on the predicted winds respect some credible bounds estimated from archived weather reports. The uncertainty sets are updated each time a new observation is received by excluding those values of the unknowns which give rise to predictions which are not consistent with the newly received observation. Each time the uncertainty set of the unknowns is updated, a new set of guaranteed predictions is computed accordingly. The attractive feature of this approach is that the uncertainty set of the unknowns and the set of predictions are systematically reduced at the reception of each new observation, while remaining guaranteed sets in the worst-case sense.

The idea of a combined worst-case and Monte Carlo methodology was recently proposed by Balestrino, Caiti and Crisostomi[27], [28]. It is a novel solution to the problem of choosing representative values from the uncertainty set provided by a set-membership approach. This is an important issue because such values allow one to calculate useful quantities which can be used as 'indicative' estimates within the worst-case bounds. In the previous literature, this problem has been tackled with a deterministic approach consisting of the choice of nominal values corresponding to some geometrical definition of a center of the uncertainty set - see e.g. Bai et al.[29]. Balestrino, Caiti and Crisostomi[27], [28] put forward the idea of using particle filters for constructing an approximate a posteriori Bayesian distribution over the worst-case uncertainty sets. In this way one can use representative probabilistic estimates, such as the probability of conflict and the expected time of arrival, within the worst-case bounds. Balestrino, Caiti and Crisostomi[27], [28] developed combined Monte Carlo and set-membership algorithms for the case of a linear model. In this case study, we do not restrict the scope to linear models because our aim is to employ the non-linear performance model of BADA[17].

III. The case study

In a TMA sector, aircraft, towards the end of their flight, descend from cruising altitude, around 30000 *ft* and above, to the entry points of the Approach Sector of the destination airport, which are typically between 5000 *ft* and 15000 *ft* - see e.g. Lecchini-Visintini et al.[30]. Here, we specifically address the problem of performing trajectory prediction for an aircraft on a leg of flight composed of the following three phases: an initial phase in level flight at 30000 *ft*, followed by a descent to 10000 *ft* and a final phase again in level flight at 10000 *ft*.

The intent of the aircraft is specified as follows. The aircraft is initially at 30000 *ft* in level flight and will continue to travel maintaining constant heading. In the coordinate system of Figure 1, which has the x-axis aligned to the aircraft's heading, the leg of flight of interest begins at ($x = 0$ *nmi*, $h = 30000$ *ft* (9144 *m*)). The aircraft will begin the descent phase when $x = 10$ *nmi* (18.52 *km*) is reached. The descent phase will be executed at controlled vertical speed, or, equivalently, at controlled Rate Of Climb or Descent (ROCD). Here it is assumed that during the descent phase the pilot will use the Vertical Navigation (VNAV) system to follow a desired vertical path which has been issued by ATC. The aircraft will resume level flight when the altitude of 10000 *ft* (3048 *m*) is reached. The end of the leg of flight of interest is set at ($x = 110$ *nmi* (203.72 *km*), $h = 10000$ *ft*).

We assume that the specified intent will be executed with no navigation errors. This assumption implies that: (i) the aircraft will fly maintaining null heading error throughout, (ii) the aircraft will begin the descent phase exactly when $x = 10$ *nmi* is reached, and (iii) the aircraft will execute the vertical path issued by ATC with no vertical navigation errors. In this work we will focus on the prediction of the displacement of the aircraft along the x-axis. Uncertainty in the prediction of the aircraft trajectory will arise from the lack of knowledge of the exact mass of the aircraft in the prediction model, from the errors between the predicted and the actual winds encountered by the aircraft and from the observation errors.

Our case study represents a typical operational scenario in current ATC practice. Heading instructions, are commonly used by air traffic controllers to guide aircraft in Terminal Areas. Heading instructions are often referred to as "radar vectors" because they simply correspond to issuing a direction to the heading of the aircraft on the air traffic controller's radar screen [31]. Controllers can issue vertical speed profiles to aircraft in order to meet operational constraints on altitude, e.g. be at or below a specified flight level at a certain waypoint [32], [33]. In particular, in terminal airspace, this can be done in order to meet traffic flow management constraints, as discussed in Mondoloni et al.[34] The presence of uncertainty in the forward displacement of the aircraft during a descent at controlled vertical speed is discussed also in Mondoloni and Ballin[35], where the need for updating descent trajectory predictions using radar measurements is pointed out.

It is worth pointing out that, while maintaining constant heading, the aircraft would undergo a drift displacement in the direction orthogonal to the x-axis due to the action of the components of the wind in that direction. However, in this situation, the motion of the aircraft in the forward direction and the motion of the aircraft in the lateral direction are decoupled. In this study, we focus on the prediction of the

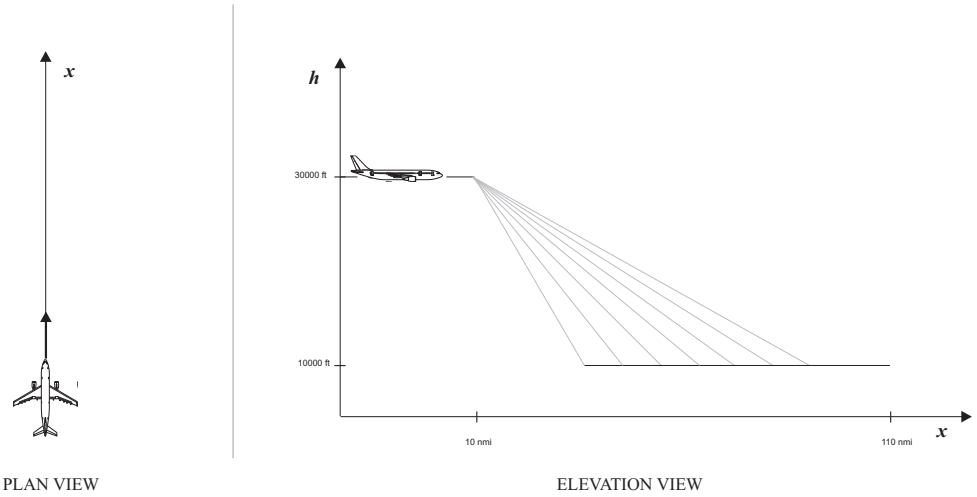

Fig. 1. The leg of flight of interest in the x (forward displacement) and h (altitude) coordinate system adopted in the case study. Uncertainty in the prediction of the displacement of the aircraft along the x-axis is due to the action of the winds, inexact knowledge of the mass of the aircraft and observation errors.

forward displacement of the aircraft only. It is straightforward to apply the same procedures to predict the lateral drift. Hence, for conciseness, this part is omitted in the presentation of the case study.

In the remainder of this section we introduce the models employed in this case study.

A. The wind model

In our case study the largest deviations from nominal predictions are caused by the action of the wind. Nominal wind predictions are usually available. However, an error in the prediction of the winds should still be taken into account in order to provide reliable trajectory predictions. A convenient choice is to consider the wind as having two components: a nominal one, which corresponds to the predicted wind, plus an additive component, which corresponds to the prediction error. We model the additive error as a zero mean random variable. Just for the sake of simplicity, we will assume that the nominal wind is zero. In our approach, a non-zero nominal component of the wind could be easily taken into account and be included in the model as a known offset to the mean of the 'stochastic wind'.

We characterize the stochastic component of the wind with the statistics provided by Chaloulos and Lygeros [12], which in turn are based on available accuracy studies of the Rapid Update Cycle (RUC) forecast model [36], [37]. We assume that the wind remains constant at constant altitude. Hence, our model implies that the aircraft in level flight encounters a constant wind, and that the wind becomes instead a function of the altitude during the descent phase. This assumption reflects the fact that winds at the same altitude are far more correlated than winds at different altitudes[12]. In particular, this assumption can be expected to be realistic for the relatively small distances traveled in our case study.

In our case study, only the component of the wind velocity in the direction of the x-axis is relevant and we will denote

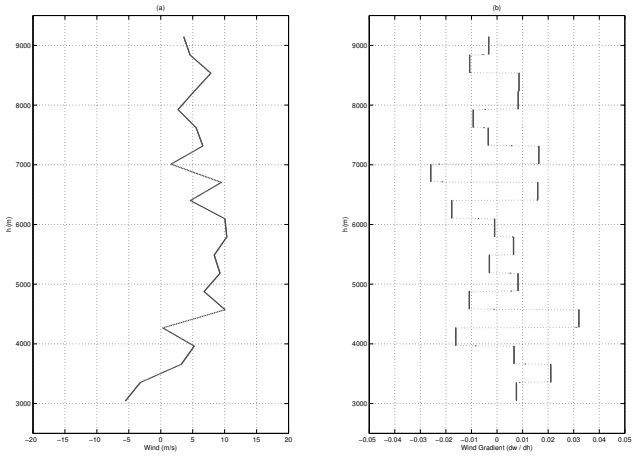

Fig. 2. (a) a possible realization of the wind profile; (b) the corresponding realization of the gradient of the wind with respect to altitude.

it with w. In order to generate samples of the wind velocity we consider 21 wind levels equally spaced every 1000 ft in an altitude grid $h_i^*, i = 1,..,21$ from 10000 ft to 30000 ft. The values of the stochastic component of the wind at these altitudes are generated as samples from a truncated multivariate Gaussian distribution having standard deviation $\sigma_{wind} = 6\ m/s$ and covariance matrix Σ_{wind} which reproduces the vertical correlation of the wind provided by Chaloulos and Lygeros [12]. The support domain of the multivariate Gaussian distribution is truncated in such a way that the winds, and the difference between the winds at adjacent altitude levels, respect the following bounds:

$$\begin{cases} |w(h_i^*)| \leq 20\ m/s & \forall i = 1,..,21 \\ \left|w\left(h_{i+1}^*\right) - w(h_i^*)\right| \leq 20\ m/s & \forall i = 1,..,20 \end{cases} . \quad (1)$$

Notice that these bounds correspond to truncating the Gaussian distribution beyond $3\,\sigma_{wind}$ (similar but less conservative bounds have been used in Kitsios and Lygeros [38]). The

values of the winds at intermediate altitudes are generated by linear interpolation. A wind profile generated by our model is displayed in Figure 2. Notice that, since the wind velocity changes linearly between two adjacent levels, the gradient of the wind with respect to the altitude is piecewise constant.

Let us recall that the assumption that the disturbances belong to a bounded set is required otherwise set-membership techniques cannot provide guaranteed predictions. In the case of the wind, it is important to introduce bounds also on the difference between the winds at adjacent altitude levels because the gradient of the wind has an important role in the aircraft performance model (see the following subsection).

Wind models, more complex than the one employed here, can be easily introduced without affecting the applicability of our approach. Worst-case computations require only the values of the bounds on the winds introduced above. Monte Carlo methods require only that many simulations should be run of the adopted probabilistic wind model, such as the one used here, or a more complex one, such as the one used by Chaloulos and Lygeros[12].

B. The aircraft performance model

In level flight the motion of aircraft is described sufficiently well by a simple kinematic model. Our assumption of null heading error simplifies the model to the following equation for the displacement of the aircraft along the x-axis:

$$x(k+1) = x(k) + V_{TAS} \cdot \Delta t + w \cdot \Delta t \tag{2}$$

where Δt is the discretization step, w is the wind speed as discussed in the previous subsection, and V_{TAS} is the True Air Speed of the aircraft. Standard airline procedures provide that aircraft maintain a constant Calibrated Air Speed (V_{CAS}) between 10000 ft until Mach transition altitude (about 30000 ft), e.g. page C28 of [17]. In this work, we specifically refer to the aircraft performance model developed in BADA (Base of Aircraft DAta) [17]. The True Air Speed V_{TAS} in level flight can be computed from the prespecified V_{CAS}, according to the equation:

$$V_{TAS} = \left[\frac{2P}{\mu\rho} \left\{ \left(1 + \frac{P_0}{P} \left[\left(1 + \frac{\mu\rho_0}{2P_0} V_{CAS}^2 \right)^{1/\mu} - 1 \right] \right)^{\mu} - 1 \right\} \right]^{1/2} \tag{3}$$

where P is the atmospheric pressure and ρ is the air density. The values of P and ρ are computed as functions of the temperature as $P = P_0 \cdot \left(\frac{Temp}{Temp_0} \right)^{-\frac{g}{k_T R}}$ and $\rho = \rho_0 \left(\frac{Temp}{Temp_0} \right)^{-\frac{g}{k_T R}-1}$. The quantities $P_0 = P_{ISA} = 101325\ Pa$, $\rho_0 = \rho_{ISA} = 1.225\ kg/m^3$ and $Temp_0 = Temp_{ISA} = 288.15\ K$ are respectively the values of pressure, density and temperature at sea level, here assumed to be equal to their International Standard Atmosphere (ISA) nominal values. In these equations $R = 287.04 m^2/\left(Ks^2\right)$ is the real gas constant for air and $k_T = -0.0065\ K/m$ is the nominal ISA temperature gradient for altitudes below the tropopause. The temperature can be computed as a function of altitude: $Temp = Temp_0 - 6.5\frac{h}{1000}$. In (3) the nominal value of μ is $2/7$. In this case study, we assume that the true airspeed V_{TAS} in level flight can be considered constant and known as given from the above equations. In addition, for notational convenience, from now on V_{TAS} will be simply denoted as v.

The performance model for the descent phase is more complex. In accordance with BADA[17], we can assume that during the descent the aircraft follows a nominal thrust profile which depends on the altitude. Since we also assume that the aircraft follows a known vertical profile with no navigation errors, we actually fall under case (b) on page C7 of the BADA user manual[17]. In this case, ROCD, the altitude and the thrust in the BADA performance model become known at each step. The equations of the performance model are:

$$\begin{cases} x(k+1) &= x(k) + v(k) \cdot \cos\gamma(k) \cdot \Delta t + w(h(k)) \cdot \Delta t \\ h(k+1) &= h(k) + ROCD(k) \cdot \Delta t \\ \gamma(k) &= \arcsin\left(ROCD(k)/v(k)\right) \\ v(k+1) &= \left[\dfrac{T(h(k)) - D(h(k), v(k), m)}{m} \right] \cdot \Delta t \\ & \quad -g \cdot \sin\gamma(k) \cdot \Delta t - WG(h(k)) \cdot \\ & \quad \cdot ROCD(k) \cdot \cos\gamma(k) \cdot \Delta t + v(k) \\ m &= \text{const} \end{cases} \tag{4}$$

where T is the thrust, D is the drag, g is the gravitational acceleration (9.81 m/s^2), γ is the flight path angle and WG is the gradient of the wind with respect to the altitude. The system of equations is written emphasising the role of ROCD. In the model, we have introduced the approximation that the mass of the aircraft remains constant during the descent. This is a good approximation since aircraft's descent is mainly due to gravity and only a very small amount of fuel is burned during a descent.

The descent thrust T and the drag D in (4) can be computed using the equations reported in BADA [17]. These equations are recalled here for completeness and because we will use them in the derivations of the prediction algorithms. In order to simplify the notation, we use the fact that the aircraft follows a prespecified altitude profile and treat the dependencies on altitude simply as dependencies on time, e.g. the thrust will be denoted by $T(k)$ instead of $T(h(k))$. We have: $T(k) = C_{Tdes,high} \times T_{maxclimb}(k)$, where $T_{maxclimb}(k)$ for a jet engine type is given by $T_{maxclimb}(k) = C_{Tc1} \times \left(1 - \frac{h(k)}{C_{Tc2}} + C_{Tc3} \times h^2(k)\right)$, and $D(k) = \frac{1}{2} C_D(k) \cdot \rho(k) \cdot v^2(k) \cdot S$, where the drag coefficient $C_D(k)$ is computed as $C_D(k) = C_{D0,CR} + C_{D2,CR} \times \left(C_L(k)\right)^2$ and the lift coefficient $C_L(k)$ is given by $C_L(k) = \frac{2 \cdot m \cdot g}{\rho(k) \cdot v^2(k) \cdot S \cdot cos\phi(k)}$. The lift coefficient is determined assuming that the flight path angle is zero [17]. Moreover, in our case the correction for the bank angle $\phi(k)$ can be neglected. The coefficients C_{Tc1}, C_{Tc2}, C_{Tc3}, $C_{D0,CR}$, $C_{D2,CR}$ and S (wing reference area) depend on the aircraft and their values for different models can be found in BADA [17].

In our study case, we assume that the unknown quantity in this model is the mass m. The other unknowns are the wind velocity w, and the gradient of the wind WG, as discussed in the previous subsection. Let us finally remark that the performance model for the descent phase is nonlinear, as it is particularly evident in the fourth equation where the thrust and the drag are complicated functions of the aircraft speed, mass and altitude.

C. The observation model

We assume that radar observations are received every 6 *sec*. In this case study, only the observations of the x-component of the position of the aircraft are considered.

We assume that the likelihood of observation errors has the form of a Gaussian density function with zero mean and variance $\sigma^2_{pos} = 500\ m^2$ truncated at $2\,\sigma_{pos}$. The fact that the likelihood of observation errors has a bounded domain implies that each observation determines an interval on the x-axis of length $4\,\sigma_{pos}$, centered on the observation itself, in which the x-component of the position of the aircraft is guaranteed to be.

We assume that also the aircraft airspeed is observed. (Let us recall that the airspeed is constant and known in level flight but will change according to the equations of the performance model during the descent.) This assumption is justified if Mode-S[2] or ADS-B[3] broadcast systems are in operation. However, it is not a crucial assumption. In fact, we will show that if airspeed measurements are available, then they can be used to improve predictions. In this case, we assume that the likelihood of the air speed measurement errors has the form of a Gaussian density function with zero mean and variance $\sigma^2_{speed} = 10\ (m/s)^2$ truncated at $2\,\sigma_{speed}$.

Let us recall that the assumption that observation errors belong to a bounded set is required otherwise set-membership techniques cannot provide guaranteed predictions. Such an assumption corresponds to assuming that outliers, i.e. completely wrong observations, never occur, or, if they occur, that they are detected and discarded.

IV. Worst-case prediction algorithms

In this section we construct the algorithms for computing worst-case predictions for our case study. As stated above, we employ a set-membership approach in which the worst-case prediction sets are updated recursively. The contributions on the set-membership approach in the literature deliver several algorithms for linear and uncertain linear systems - see e.g. Schweppe [23], Bertsekas and Rhodes [24], Chisci et al. [25], Polyak et al.[26]. Here we develop specific algorithms to implement a set-membership approach with the full nonlinear performance model of the previous section.

The essence of the set-membership approach is the recursive computation and update of three sets: the prediction set, the correction set and the corrected set. The prediction set contains all the predictions which are consistent with the values in the uncertainty sets of the current states and of the unknowns. The correction set is computed when a new observation is received and contains all the values of the states which, according to the observation model, are consistent with the new received observation. The corrected set is also computed each time a new observation is received and is defined as the intersection between the prediction set, calculated at the time of the new observation but starting from the values in the uncertainty sets of the states and of the unknowns at the time of the last received observation, and the correction set corresponding to the new observation. The corrected set represents the set-membership estimate of the state and is the set of initial conditions for new, updated, prediction sets.

In this section we introduce some specific notation. This notation will be used throughout the remainder of the paper. To exemplify the notation, let us consider the forward displacement of the aircraft $x(k)$. We use * to denote observations, i.e. an observation of the forward displacement at time k is denoted by $x^*(k)$. The time indices k and k^-, with $k > k^-$, denote, respectively, the current time instant and the time instant of the last received observation. The symbol $\underline{\hat{x}}(k^- + d|k^-)$ ($\bar{\hat{x}}(k^- + d|k^-)$) denotes the lower (upper) bound of the prediction set of the forward displacement at time $k^- + d$ given the values in the corrected sets of the states and of the unknowns at the time instant k^-. If a new observation is received at time k, then the symbol $\underline{x}(k|k)$ ($\bar{x}(k|k)$) denotes the lower (upper) bound of the corrected set of the forward displacement at time step k. Similarly, for a variable like the mass m, which is uncertain but does not change in time, the symbol $\underline{m}(k)$ ($\overline{m}(k)$) denotes the lower (upper) bound of its uncertainty set calculated on the basis of the observations received up to time k.

A. Level part of the flight

In the level part of the flight, the only relevant equation is (2) (recalled here for convenience)

$$x(k+1) = x(k) + v \cdot \Delta t + w \cdot \Delta t$$

in which the airspeed v is constant and known as explained in the description of the aircraft performance model. The unknowns are the initial displacement x_0 and the wind w. Let us recall that the wind in level flight is assumed to be constant and uncertain within known bounds - see (1). The initial displacement x_0 is also uncertain but within known bounds which can be inferred from the first received observation in accordance to the observation model. Therefore we have:

$$\begin{cases} x_0 \in [\underline{x}_0(0) \quad \bar{x}_0(0)] \\ w \in [\underline{w}(0) \quad \overline{w}(0)] \end{cases} . \tag{5}$$

As already mentioned, the time indices in the bounds express the fact that the future observations will reduce the uncertainty intervals.

The prediction set of the forward displacement based on the information collected up to the time instant of the last received observation (k^-) is obtained by computing the maximum and minimum value that the forward displacement can assume at any successive time instant $k^- + d$. These values are given by:

$$\begin{cases} \underline{\hat{x}}(k^- + d|k^-) = \underline{x}_0(k^-) + (k^- + d) \cdot (v + \underline{w}(k^-)) \cdot \Delta t \\ \bar{\hat{x}}(k^- + d|k^-) = \bar{x}_0(k^-) + (k^- + d) \cdot (v + \overline{w}(k^-)) \cdot \Delta t \end{cases} . \tag{6}$$

Here, the time $k^- + d$ can not exceed the instant when $x = 10$ *nmi* is reached, because at that point different prediction equations based on the descent model have to be used. These equations will be described in the next subsection.

If at current time k a new observation $x^*(k)$ is received, then a correction set and a corrected set can be computed. The correction set is defined by the observation model. In our case we have: $x(k) \in [x^*(k) - 2\sigma_{pos} \quad x^*(k) + 2\sigma_{pos}]$. The corrected set $[\underline{x}(k|k) \quad \overline{x}(k|k)]$ is the intersection between the correction set and the predicted set at time k calculated starting from the uncertainty sets at time instant k^- of the last received observation. Therefore we have:

$$\begin{cases} \underline{x}(k|k) &= \max\left\{x^*(k) - 2\sigma_{pos}, \underline{\hat{x}}(k|k^-)\right\} \\ \overline{x}(k|k) &= \min\left\{x^*(k) + 2\sigma_{pos}, \overline{\hat{x}}(k|k^-)\right\} \end{cases} . \quad (7)$$

In turn, the reduction of the uncertainty on the forward displacement allows one to reduce the uncertainty intervals of the other unknowns. We have:

$$\begin{cases} \underline{w}(k) &= \max\left\{\frac{\underline{x}(k|k) - \overline{x}_0(k^-) - k\cdot v\cdot\Delta t}{k\cdot\Delta t} \ , \ \underline{w}(k^-)\right\} \\ \overline{w}(k) &= \min\left\{\frac{\overline{x}(k|k) - \underline{x}_0(k^-) - k\cdot v\cdot\Delta t}{k\cdot\Delta t} \ , \ \overline{w}(k^-)\right\} \\ \underline{x}_0(k) &= \max\left\{\underline{x}(k|k) - k\cdot\left(v + \overline{w}(k^-)\right)\cdot\Delta t \ , \ \underline{x}_0(k^-)\right\} \\ \overline{x}_0(k) &= \min\left\{\overline{x}(k|k) - k\cdot\left(v + \underline{w}(k^-)\right)\cdot\Delta t \ , \ \overline{x}_0(k^-)\right\} \end{cases} . \quad (8)$$

It follows from equations (8) that at each observation step the uncertainty about the initial displacement and the wind cannot increase. The proof of the previous equations can be found in the Appendix. These updated values allow one to calculate more accurate predictions for the future time instants until a new observation is received and the correction cycle is repeated.

We have proposed here a simple and efficient solution that takes advantage of the fact that the two unknowns, the initial displacement and the wind are constant. The same problem could have been approached using more general and complex algorithms, as for instance the one proposed by Chisci et al. [25] for discrete-time linear systems.

B. The descent phase

In the descent phase the computation of the guaranteed predicted set of the forward displacement is more complex because there is more uncertainty (i.e. the effects of an unknown mass and of the winds) and because the aircraft performance model (4) becomes non-linear. Here we consider a solution strategy where the problem of determining the worst-case prediction sets is formulated as the constrained optimization problem of finding the extreme values of all possible aircraft forward displacements which are consistent with the corrected sets of the states and of the unknowns at the time of the last received observation.

Hence we have:

$$\begin{array}{rcll} \overline{\hat{x}}(k^- + d|k^-) &= & \max & x(k^- + d) \quad \text{given by (4)} \\ & & m \in [\underline{m}(k^-) \quad \overline{m}(k^-)] & \\ & & w(h_i^*) \ i = 1,..,21 & \text{subject to (1)} \\ & & x(k^-) \in [\underline{x}(k^-|k^-) \quad \overline{x}(k^-|k^-)] & \\ & & v(k^-) \in [\underline{v}(k^-|k^-) \quad \overline{v}(k^-|k^-)] & \end{array} . \quad (9)$$

A similar problem must be solved to find the minimum forward displacement $\underline{\hat{x}}(k^- + d|k^-)$.

In general, it is hard to find a solution to a problem like (9). However, here we succeed in finding a conservative but efficient strategy for approaching the solution. Our strategy approaches the optimization problem by handling one variable at a time and, in doing so, it exploits the structure of the problem. In particular, we will make use of the following fact: If we assume that the winds $w(h_i^*) \ i = 1,..,21$ are given then a conservative way of approaching $\overline{\hat{x}}(k^- + d|k^-)$ for a given profile of winds is to compute the worst-case (highest possible) airspeed at each step. In fact, we have assumed that $v(k)\sin\gamma(k) = ROCD(k)$ is given and fixed. Therefore, a higher value of $v(k)$ would correspond to a lower value of $\sin\gamma(k)$ and eventually, in the range of interest of small positive values of γ, to a higher value of the term $v(k)\cos\gamma(k)$ which appears in the first equation of (4). Hence, a higher value of $v(k)$ would cause, as a consequence, a larger forward displacement. Obviously a similar argument holds for the computation of the minimum forward displacement $\overline{\hat{x}}(k^- + d|k^-)$. In this case the lowest values of $v(k)$ would give the smallest forward displacement.

The strategy for approaching the solution of (9) is described in detail below.

Step 1: We find the worst-case values of the mass m which give the highest or lowest possible velocity at each step. Let us re-write the fourth equation of (4) in order to make the dependence of the drag on the mass and the velocity explicit:

$$v(k+1) = v(k) + \left[\frac{T(k)}{m} - \frac{C_{D0,CR}\rho(k)v^2(k)S}{2m} - \frac{2C_{D2,CR}mg^2}{\rho(k)v^2(k)S}\right]\Delta t - g\cdot\sin\gamma(k)\cdot\Delta t - \\ - WG(h(k))\cdot ROCD(k)\cdot\cos\gamma(k)\cdot\Delta t . \quad (10)$$

In the above equation, the maximum $v(k+1)$ is obtained when the mass takes one of the three possible values: $m^{max}(k) = \underline{m}(k^-)$, $m^{max}(k) = \overline{m}(k^-)$ or

$$m^{max}(k) = \frac{v(k)}{2g}\sqrt{\frac{\rho(k)S\left(C_{D0,CR}\rho(k)v^2(k)S - 2T(k)\right)}{C_{D2,CR}}} . \quad (11)$$

The minimum of $v(k+1)$ is instead obtained when the mass takes one of the two possible extreme values: $m^{min}(k) = \underline{m}(k^-)$, $m^{min}(k) = \overline{m}(k^-)$ (see the Appendix).

Step 2: Employing the worst-case values of the mass derived in Step 1 and under the assumption that the wind profile $w(h_i^*) \ i = 1,..,21$ is given, we compute a conservative estimate of $\overline{\hat{x}}(k^- + d|k^-)$. To start with, we consider the initial conditions $x(k^-)$ and $v(k^-)$. The initial displacement $x(k^-)$ is simply an additive term in the first equation of (4). Therefore the maximum and minimum values of the initial interval $[\underline{x}(k^-|k^-) \quad \overline{x}(k^-|k^-)]$ are the worst-cases initial conditions for the maximum and minimum value of the future forward displacements. The airspeed must be treated in a different way. We grid $[\underline{v}(k^-|k^-) \quad \overline{v}(k^-|k^-)]$ and for each value of $v(k^-)$ in the grid we compute the airspeed at the $k^- + 1$ time instant according to (10) in which we set the mass to $m^{max}(k^-)$. We then keep the maximum value of $v(k^- + 1)$ which is an upper bound of all possible values of the airspeed at time $k^- + 1$. The procedure is then repeated

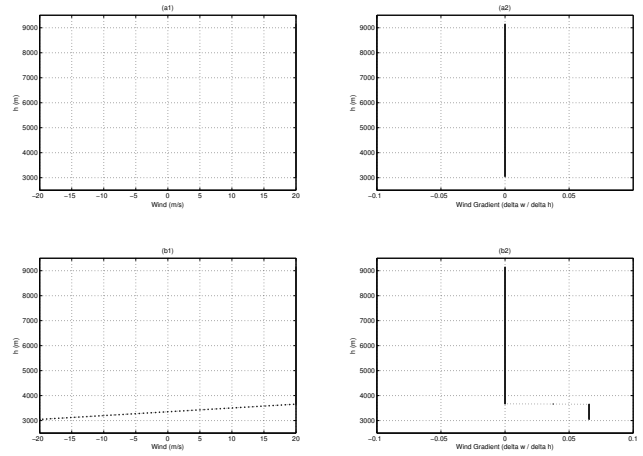

Fig. 3. (a1-a2) worst-case wind profile that gives the maximum forward displacement; (b1-b2) worst-case wind profile that gives the maximum airspeed at the end of the prediction horizon.

iteratively at each time step in order to obtain the maximum of all possible values of the airspeed at each step of the prediction horizon $[k^-, k^-+1, \ldots, k^-+d]$. A conservative estimate of $\overline{\hat{x}}(k^-+d|k^-)$ is then obtained using the first equation of (4) in which the highest possible airspeeds appear at each step. In order to obtain a conservative estimate of $\underline{\hat{x}}(k^-+d|k^-)$ we repeat the process by calculating the lowest possible airspeed at each step. The solution is conservative because we act as if the mass was allowed to change at each step. Conservatism is also introduced by the fact that the worst-case airspeeds are computed sequentially at each time step instead of being found by optimizing the airspeed profile at once over the whole prediction horizon.

Step 3: In the last step we compute the worst-case values of the wind profile. The winds affect the first equation of (4) and the fourth equation of (4) (i.e. (10)) through the winds' gradients. Here the objective is to compute the sequence of winds which gives the maximum and minimum forward displacements, at all the altitudes that are covered by the given prediction horizon $[k^-, k^-+1, \ldots, k^-+d]$, and are consistent with the constraints in (1). We achieve this objective by using the Sequential Quadratic Programming method for constrained nonlinear optimization. (We employed the MATLAB implementation of SQP, see: `'fmincon'` in MATLAB.) In the optimization procedure, we compute the worst-case values of the final forward displacement as described in Steps 1 and 2 for each candidate wind profile produced by the optimization function. We found that the solution of this optimization problem is a wind constantly equal to its maximum possible value, for $\overline{\hat{x}}(k^-+d|k^-)$, or constantly equal to its minimum possible value for $\underline{\hat{x}}(k^-+d|k^-)$ (see Figure 3.a1-a2). We tested extensively this solution by varying the initial instant and the length of the prediction horizon and by varying the initial guess of the wind profile at the start of the wind optimization procedure.

The above procedure allows one to compute the guaranteed prediction set of the forward displacement during the descent. When a new observation is received the prediction set is intersected with the corresponding correction set in order to obtain a new corrected set (in the same way as it was done in (7)). One important aspect of the procedure is that the worst-case occurrence of the wind profile turns out to be independent from the initial instant and the length of the prediction horizon and therefore is known in advance. Hence, there is no need to perform the optimization of the wind profile online.

Our procedure, with minimal modifications, can be used also to compute the prediction sets $[\underline{v}(k^-+d|k^-) \quad \overline{v}(k^-+d|k^-)]$ of the airspeed. Although airspeed predictions may not be as directly useful as the predictions of the future forward displacement from the point of view of ATC, the reason for calculating prediction sets for the airspeed is that they are used to compute the corrected sets $[\underline{v}(k|k) \quad \overline{v}(k|k)]$ each time an airspeed observation is received. In principle, the uncertainty sets for the initial condition of the airspeed in (9) can be chosen to be simply the correction sets corresponding to the last received observation. However, by calculating prediction and corrected sets also for the airspeed one obtains smaller uncertainty sets of the initial condition and eventually better predictions of the future displacement. The corrected sets $[\underline{v}(k|k) \quad \overline{v}(k|k)]$ are obtained through the usual operation of intersection between the prediction sets and the correction sets of the received observations. The only required modification in Steps 1-3 is that the optimization objective $\overline{x}(k^-+d|k^-+d)$ is replaced by the new objective $\overline{v}(k^-+d|k^-)$ in Step 3. In this case we found that the solution is a wind constantly equal to its maximum possible value until the last 2000 ft of the descent covered by the prediction horizon $[k^-, k^-+1, \ldots, k^-+d]$. In the last 2000 ft of descent the wind gradient switches from zero to its maximum possible value and, as a consequence, the wind switches from its maximum to its minimum possible value (Figure 3.b1-b2). The intuitive explanation of this solution is that the gradient of the wind has a strong effect in the fourth equation of (4) but cannot be equal to its maximum value for more than 2000 ft of descent, otherwise the growth of the wind would violate (1). The solution has the same desirable property of the solution for the worst-case position: it is independent from the initial instant and from the length of the prediction horizon. Therefore, there is no need to perform the optimization of the wind profile online.

The update of the uncertainty interval $[\underline{m}(k^-) \quad \overline{m}(k^-)]$ of the mass of the aircraft can be done in a similar way as the update of the uncertainty interval of the initial displacement was done during the first level leg of the flight. However, in this case the model is too complex to give rise to explicit update equations like (8). In order to update $[\underline{m}(k^-) \quad \overline{m}(k^-)]$ when a new observation $x^*(k)$ is received we can employ the following general procedure. We start by setting $m = \underline{m}(k^-)$ in the fourth equation of (4) and compute the minimum and maximum possible positions (following Steps 2 and 3) at the time of observation $x^*(k)$ starting from the beginning of the descent. If the so-obtained interval of forward displacements at the time of observation $x^*(k)$ does

not intersect with the corrected set $[\underline{x}(k|k) \quad \overline{x}(k|k)]$ then the value $m = \underline{m}(k^-)$ can be eliminated from the uncertainty set of the mass because it certainly gives rise to a forward displacement which is inconsistent with the guaranteed uncertainty set of the forward displacements. The procedure is repeated for a new value of the mass in $[\underline{m}(k^-) \quad \overline{m}(k^-)]$, increased by one quantization step from the previous one, until a value of the mass which gives rise to an interval of forward displacements that intersects $[\underline{x}(k|k) \quad \overline{x}(k|k)]$ is reached. This value of the mass is then the updated $\underline{m}(k)$. A similar procedure is performed starting from $m = \overline{m}(k^-)$ and the updated $[\underline{m}(k) \quad \overline{m}(k)]$ is eventually obtained.

V. Combining the Monte Carlo and worst-case approaches

In the previous section, the implementation of a set-membership approach with the use of the non-linear aircraft performance model entailed the development of tailored algorithms. By contrast, it is very straightforward to implement Monte Carlo algorithms, even in a non-linear, non-Gaussian framework, because it simply requires simulations of the performance model to be run. In the following we first recall the essence of sequential Monte Carlo methods and then introduce our combined worst-case and Monte Carlo approach.

In sequential Monte Carlo algorithms, predictions are made by generating an empirical distribution of the most probable future trajectories. Each predicted trajectory is represented by a 'particle'. In our case, each particle is a vector with six elements:

$$s^{(p)}(k)=\left[x^{(p)}(k),\ h^{(p)}(k),\ v^{(p)}(k),\ m^{(p)}(k),\ w^{(p)}(k),\ WG^{(p)}(k)\right]^T$$

where the superscript p refers to the p_{th} particle with $p = 1,\ldots,N$. Notice that s includes both the states of the aircraft model $x,\ h,\ v$, and the unknowns $m,\ w,\ WG$. In the prediction phase, the states evolve according to the dynamics of the aircraft performance model. The elements representing the unknowns evolve according to the artificial dynamics which will be described in the following paragraphs. Each time a new observation is received, the population of N particles is rejuvenated using a resampling scheme. In brief, this corresponds to raising the number of trajectories which are given higher likelihood by the observation model and to discarding trajectories with low likelihood. The so-obtained predictions constitute an empirical distribution of the most probable future trajectories, given the priors on the unknowns and the received observations, and can be used to obtain various estimates, such as the expected time of arrival, by simply taking the sample average of the quantity of interest over the population of particles. The resampling step is the key step in implementing a Monte Carlo approach because it guarantees that a sufficient statistical significance of the population of particles is maintained throughout. In this work we have adopted the 'Residual Resampling' scheme of Van der Merwe et al. [19] which has a simple algorithmic implementation. More detailed descriptions of the sequential Monte Carlo approach can be found in Blom et al. [13], Van der Merwe et al. [19], Doucet et al. [20], Arulampalam et al. [21], and in the survey paper by Künsch[22].

In the implementation of the sequential Monte Carlo approach it is required to generate sequential realizations of the winds according to the model of Section III-A. In particular, the realizations of the future winds $\left[w\left(h^*_{i+1}\right) \ldots\ w(h^*_{21})\right]$, which will be encountered by a particle which is currently at wind level i, must be generated using the distribution of $\left[w\left(h^*_{i+1}\right) \ldots\ w(h^*_{21})\right]$ conditioned on the realization of the previous winds $[w(h^*_1)\ \ldots\ w(h^*_i)]$. In our case, the conditional distribution of $\left[w\left(h^*_{i+1}\right) \ldots\ w(h^*_{21})\right]$ given $[w(h^*_1)\ \ldots\ w(h^*_i)]$ is a truncated Gaussian distribution with mean value and covariance given respectively by

$$\Sigma_{(2,1)}\Sigma^{-1}_{(1,1)}\left[w\left(h^*_1\right)\ \ldots\ w\left(h^*_i\right)\right]^T, \quad \text{and} \quad \Sigma_{(2,2)}-\Sigma_{(2,1)}\Sigma^{-1}_{(1,1)}\Sigma_{(1,2)}$$

in which the matrices $\Sigma_{(i,j)}$ are the following partitions of the wind covariance matrix Σ_{wind}

$$\Sigma_{wind} = \begin{bmatrix} \Sigma_{(1,1)} & \Sigma_{(1,2)} \\ \Sigma_{(2,1)} & \Sigma_{(2,2)} \end{bmatrix}$$

with $\Sigma_{(1,1)}$ and $\Sigma_{(2,2)}$ having dimensions $i \times i$ and $(21-i) \times (21-i)$ respectively, see e.g. MacKay[39]. In order to reduce the amount of computation it is possible to introduce the approximation that, instead of all past winds $[w(h^*_1)\ \ldots\ w(h^*_i)]$, only the last few ones are used in the above expressions. In our case this approximation is very reasonable because the vertical correlation decays exponentially with altitude[12].

In our model, some of the unknowns have constant values. These are: the mass m during the descent phase, the wind w in level flight, and the wind gradient WG during the descent phase, which is piecewise constant over intervals of 1000 ft. In the estimation of unknowns, sequential Monte Carlo methods treat fixed unknowns as if they were state variables with null dynamics. However, in this case the estimate becomes very ill-conditioned. The best way of adapting sequential Monte Carlo methods to deal with the estimation of constant unknowns is still an open problem. In order to reduce the ill-conditioning of the problem, it is common practice to add some artificial dynamics to increase the variability in the population of particles which represents the constant unknown. The simplest implementation of this technique is the inclusion of an additive stochastic disturbance. In this way, the dynamics of a constant unknown such as, for instance, the mass becomes:

$$m^{(p)}\left(k+1|k^-\right) = m^{(p)}\left(k|k^-\right) + \eta^{(p)}_{mass}(k) \qquad (12)$$

where $\eta_{mass}(k)$ is zero-mean white noise. This simple solution was introduced by Gordon et al. [18]. The rationale behind this technique is that particles representing the constant unknown can assume different values and, when an observation is received, those with low likelihoods are discarded. The updated particles approximate the empirical distribution of the most probable values given the received observations. There have been proposed more sophisticated solutions which rely on Markov chain Monte Carlo methods to construct the artificial stochastic dynamics, see Lee and Chia[40], and Andrieu and Doucet [41]. The solution

illustrated in (12) is simple and computationally fast and has been adopted in our case study for the estimate of all the constant unknowns.

We now provide a schematic description of our combined sequential Monte Carlo and worst-case prediction algorithm.

COMBINED SET-MEMBERSHIP AND SEQUENTIAL MONTE CARLO ALGORITHM

1) **Initialization:**
   a) **set-membership**
   the initial uncertainty sets of the states and of the unknowns are determined on the basis of existing knowledge;
   b) **particle filter**
   the initial particles $s^{(p)}(0)$, $p = 1,\ldots,N$ are generated according to their prior distributions; the support domains of the prior distributions must coincide with the initial uncertainty sets;

2) **Prediction:**
   a) **set-membership**
   for each time instant $k^- + d$ in the prediction horizon of interest compute worst-case prediction sets $[\underline{x}(k^- + d|k^-)\ \ \bar{x}(k^- + d|k^-)]$ and $[\underline{v}(k^- + d|k^-)\ \ \bar{v}(k^- + d|k^-)]$ starting from the corrected uncertainty sets of the states and of the unknowns determined at the time of the last received observation (k^-); or starting from the initial uncertainty sets if no observations have been received yet;
   b) **particle filter**
   compute the particles $s^{(p)}(k^- + d|k^-)\ p = 1,\ldots,N$ by simulating the aircraft and wind model using the population of particles $s^{(p)}(k^-|k^-)$, $p = 1,\ldots,N$ at the time of the last received observation as initial conditions; or starting from the initial set of particles if no observations have been received yet; particles which represent parameters evolve according to the artificial dynamics as in (12);
   c) **bounds check**
   check whether each particle $s^{(p)}(k^- + d|k^-)$, $p = 1,\ldots,N$ falls in the worst-case prediction sets of time instant $(k^- + d|k^-)$; discard and recompute the particles that do not pass the check; repeat this procedure until all particles $s^{(p)}(k^- + d|k^-)$, $p = 1,\ldots,N$ belong to the worst-case prediction sets of time instant $(k^- + d)$;

3) **Correction:**
   a) **set-membership**
   if at time k a new observation is received compute corrected uncertainty sets of the states and of the unknowns;
   b) **particle filter**
   rejuvenate the population of particles $s^{(p)}(k|k)$, $p = 1,\ldots,N$ according to the adopted re-sampling scheme.

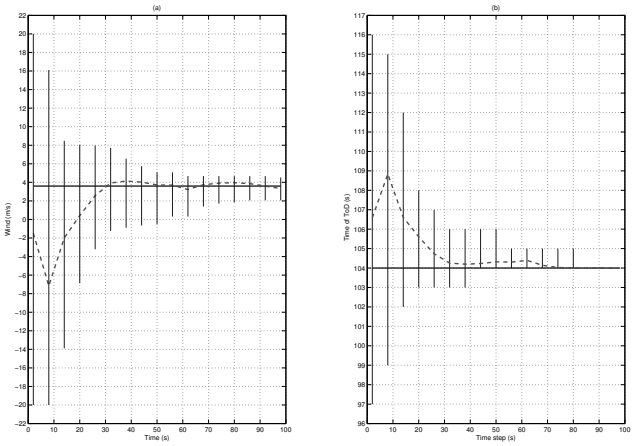

Fig. 4. (a) estimate of the wind speed during the initial phase in level flight; (b) prediction of the instant of the Top of Descent (ToD). In both figures: the bold line represents the actual value, the dashed line represents the expected value, and the vertical lines represent the worst-case estimate, or prediction, intervals.

We have already discussed in Section II that one of the advantages of our algorithm is that it provides the user with indicative estimate within the worst-case bounds. The other advantage of the algorithm is related to the use of artificial stochastic dynamics, which has been recalled above, for estimating constant unknowns in sequential Monte Carlo methods. Here the issue is that, since the artificial stochastic dynamics imposed on the constant unknowns are entirely unrelated to the adopted prediction model, it may well happen that particles representing constant unknowns eventually assume values which are physically unrealistic. In our algorithm instead a novel stage 'bounds check' performs a 'reality check' in which predictions that fall outside the worst-case bounds are rejected and recomputed. This extra step improves the parameter estimation process by including the information derived from the worst-case calculations. It is important to point out that it can be easily shown that the introduction of hard bounds in sequential Monte Carlo methods does not affect their consistency; the reader can find a proof in Lang et al. [42]. Although Lang et al. [42] introduced hard bounds for an entirely different purpose, the argument behind their consistency result remains valid when translated into our combined Monte Carlo and worst-case approach.

VI. SIMULATION EXAMPLES

In the following simulation examples we employed the parameters of an A340 aircraft in the equations of the thrust and of the drag of the aircraft performance model of Section III.C. In the simulation of the real trajectory of the aircraft, we set the mass at $m = 2.39 \cdot 10^5\ kg$, which is a value within the admissible bounds for this aircraft model, and we employed the profile of the winds shown in Figure 2. In the simulation of the performance model we set $\Delta t = 1\ sec$.

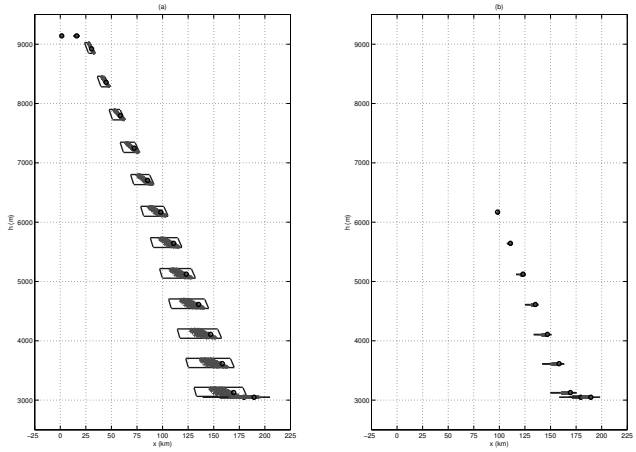

Fig. 5. Trajectory predictions drawn every 60 *sec*: (a) initial predictions; (b) half way predictions. The circles represent the real position, the grey dots represent the most probable positions, and the lines represent the worst-case prediction sets.

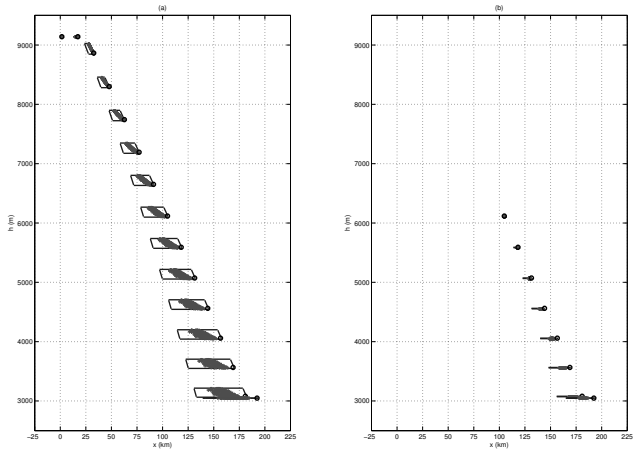

Fig. 6. Trajectory predictions in the actual worst case drawn every 60 *sec*: (a) initial predictions; (b) half way predictions. The circles represent the real position, the grey dots represent the most probable positions, and the lines represent the worst-case prediction sets.

In the implementation of the Monte Carlo approach we used $N = 200$ particles. With these settings, the computation of a combined Monte Carlo and worst-case trajectory prediction using Matlab on a laptop with a 2-GHz Intel Core 2 Duo CPU took a few tenths of a second. (It is worth pointing out the fact that no attempt has been made to optimize the code at this stage.)

In the initial phase of the flight, when the aircraft is flying at constant altitude, the wind speed and the initial displacement are the only unknowns. In the simulation of the real trajectory of the aircraft, the initial displacement was $x_0 = -40\ m$ and the wind speed was $w = 3.60\ m/s$. In Figure 4.(a) the evolution of the worst-case and Monte Carlo estimates of the wind during the first leg of the flight is displayed. In Figure 4.(b) the evolution of the prediction of the instant of the Top of Descent (ToD) is displayed. The instant of the ToD is uncertain due to the uncertainty on the wind speed and on the initial displacement. Notice how the uncertainty, in the worst-case estimates and predictions, decreases monotonically as time progresses. Notice also that the expected value estimate provided by the Monte Carlo approach is always within the worst-case intervals and that, after an initial transient due to an initial 'bad' observation, it is consistently a better estimate than the geometric center of the worst-case intervals.

In Figure 5.(a) a prediction of the trajectory of the entire leg of flight, made at the beginning of the flight when no observation have been collected yet, is displayed. In the figure, the predictions are plotted at intervals of 60 *sec*. Notice that, during the descent, the guaranteed prediction sets have a trapezoidal shape. Hence, there is uncertainty both on the horizontal displacement and the vertical position of the aircraft. The reason is that, at the beginning of the flight, even if it is known that the descent will be executed with no vertical navigation error, the time of the ToD is still uncertain. The figure displays also the empirical distribution of trajectory predictions generated by the Monte Carlo approach which represents the most probable trajectories within the guaranteed set. Notice that both the empirical distribution of the most probable trajectories and the real trajectory are always contained in the guaranteed prediction sets. In Figure 5.(b) a trajectory prediction made after the first half of the flight, when many observations have been already collected, is displayed. In this figure, the trapezoidal prediction sets have collapsed to horizontal lines. Here the reason is that the descent is executed with no vertical navigation errors. Hence, there is no uncertainty in the vertical displacement of the aircraft once the ToD has been passed. Notice how the empirical distribution of the most probable trajectories is more concentrated around the real trajectory than in the case of the initial predictions. Figure 7.(a) displays the evolution of the expected time of arrival at $x = 110\ nmi$, and of the guaranteed prediction intervals of the time of arrival, during the entire flight.

In Figure 6, the case in which the mass of the aircraft and the winds were deliberately set at their worst-case values in the simulation of the real trajectory is illustrated. In Figure 6.(a) a prediction, made at the beginning of the flight, of the trajectory of the entire flight, is displayed. Notice that the real trajectory of the aircraft turns out to be constantly on the border of the worst-case prediction sets. This means that the overestimates caused by the approximations introduced in the algorithms in Section IV.B in order to derive the worst-case bounds, are actually not very conservative. Let us remark that a more (or less) conservative worst-case solution can be obtained by tuning the worst-case bounds without affecting the computational load. Notice also that the real trajectory is far from the the empirical distribution of trajectories generated by the Monte Carlo approach. Here the reason is that these worst-case values are very unlikely to occur. In Figure 6.(b) a trajectory prediction, made after the first half of the flight, is displayed. Figure 7.(b) displays the evolution of the expected time of arrival, and of the guaranteed prediction intervals of the time of arrival. The

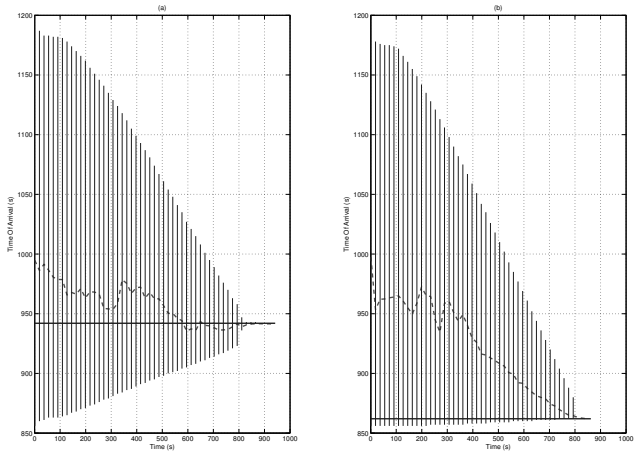

Fig. 7. Evolution of the predicted time of arrival during the flight: (a) in the case illustrated in Figure 5; (b) in the case illustrated in Figure 6. The bold line represents the actual time of arrival, the dashed line represents the expected time of arrival, and the vertical lines represent the worst-case prediction intervals.

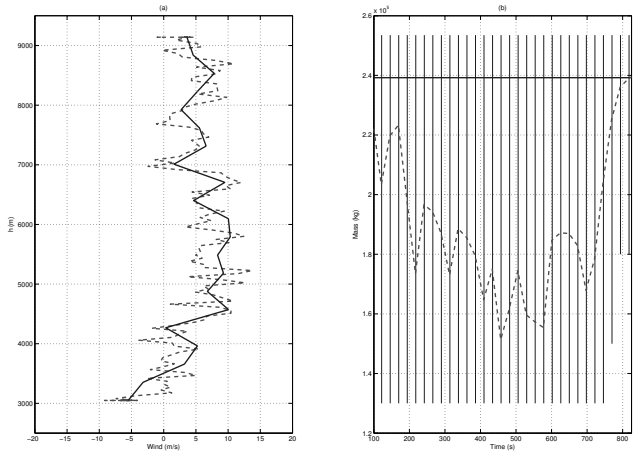

Fig. 8. (a) estimation of the wind profile: the bold line represents the the real wind profile, the dashed line represents the the expected value; (b) estimation of the mass during the descent: the bold line represents the real value of the mass, the dashed line represents the expected value, and the vertical lines represent the worst-case uncertainty intervals.

error between the expected time of arrival and the actual time of arrival is consistently larger than in Figure 7.(a) because of the unlikely values of the unknowns in this case.

In Figure 8.(a), the Monte Carlo estimate of the wind profile for the entire flight is displayed. It can be noticed that the estimation of the winds turns out to be quite accurate. Figure 8.(b) shows the evolution of the Monte Carlo and worst-case estimates of the mass of the aircraft during the descent. In our case study, the effect of the uncertainty in the mass of the aircraft on the motion of the aircraft is dominated by the effect of the uncertainty on the winds. This fact makes the estimation of the mass a difficult task. In fact, it can be noticed that both the Monte Carlo approach and the worst-case approach achieve a poor performance in estimating the mass. In particular, only a small reduction of the worst-case uncertainty intervals of the mass is achieved, towards the end of the descent.

VII. Conclusions

We have developed a case study to illustrate a novel approach which combines worst-case and Monte Carlo methods to perform model-based trajectory predictions in Air Traffic Control. Our algorithm provides: (1) the worst-case prediction sets in which the aircraft trajectory is guaranteed to belong at each future time instant, and (2) an empirical distribution of the most probable future trajectories which can be used to compute estimates such as the expected time of arrival. These predictions are calculated recursively and updated each time a new radar observation is received. We envisage that our approach will be useful to support novel conflict detection and resolution tools. An important aspect of this case study is that we have been able to employ the full non-linear aircraft performance model of BADA[17] without the need for the construction of a linearized model, which is instead a common step in many estimation and prediction methods.

Future work will focus on the application of our method to an 'open descent' where thrust and airspeed are controlled while ROCD is determined as a consequence, i.e. case (a) on page C7 of the BADA user manual[17]. On the methodological side we plan to investigate further on the use of our approach for the solution of 'difficult' estimation and prediction problems. One example of this kind of problems was the estimation of the mass in our case study. In particular, we plan to explore the combination of our approach with more sophisticated probabilistic schemes based on Markov chain Monte Carlo methods.

In current ATM systems, trajectory prediction is computed either on the basis of very simple kinematic models or on the basis of a large data set that contains information on past aircraft flights in similar operating conditions. At this stage it is still not easy to compare the computational load of our proposed approach with that of the existing system. However, although model-free approaches are much easier to compute, they do not provide the same predictions capabilities of our approach, in particular in computing the uncertainty associated with a prediction. We aim at assessing a more complete analysis of the computational performance of our approach in future work.

Acknowledgments

The authors would like to thank Angela Nuic and Costas Tamvaclis at the EUROCONTROL Experimental Centre and David Wing at NASA for pointing them to relevant papers. This work was supported by EPSRC, Grant EP/C014006/1, and by the European Commission under project iFly FP6-TREN-037180.

Appendix

Proof of Equation 8

We have that $x(k) \in [\underline{x}(k|k) \;\; \overline{x}(k|k)]$, that $x_0 \in [\underline{x}_0(k^-) \;\; \overline{x}_0(k^-)]$ and $w \in [\underline{w}(k^-) \;\; \overline{w}(k^-)]$. On the

basis of this information we want to determine the new sets $[\underline{x}_0(k) \quad \overline{x}_0(k)]$ and $[\underline{w}(k) \quad \overline{w}(k)]$.

To start with, let us re-write equation (2) as follows:

$$k \cdot w \cdot \Delta t = x(k) - x_0 - k \cdot v \cdot \Delta t,$$

from which we obtain

$$w \leq \frac{\overline{x}(k|k) - \underline{x}_0(k^-) - k \cdot v \cdot \Delta t}{k \cdot \Delta t}.$$

The equation for $\overline{w}(k)$ in (8) is eventually obtained by intersecting the set determined by the equation above and $[\underline{w}(k^-) \quad \overline{w}(k^-)]$. The equation for $\underline{w}(k)$ can be derived with similar steps.

In a similar way, if we re-write equation (2) as

$$x_0 = x(k) - k \cdot \left(v + w\left(k^-\right)\right) \cdot \Delta t$$

we obtain that

$$x_0 \leq \overline{x}(k|k) - k \cdot \left(v + \underline{w}\left(k^-\right)\right) \cdot \Delta t.$$

Using the above equation and the fact that $x_0 \in [\underline{x}_0(k^-) \quad \overline{x}_0(k^-)]$ we eventually obtain the equation for $\overline{x}_0$ in (8). Again, the equation for $\underline{x}_0$ can be obtained through similar steps.

Proof of Equation 11

From equation (10) we obtain

$$\frac{\partial v(k+1)}{\partial m} = -\frac{T(k)}{m^2} + \frac{1}{2}\frac{C_{D0,CR}\rho(k)v(k)^2 S}{m^2} - \frac{2C_{D2,CR}g^2}{\rho(k)v(k)^2 S}.$$

The value of $m^{max}(k)$ in (11) is the unique positive solution of $\frac{\partial v(k+1)}{\partial m} = 0$. We also have

$$\frac{\partial^2 v(k+1)}{\partial m^2} = \frac{2T(k)}{m^3} - \frac{C_{D0,CR}\rho(k)v(k)^2 S}{m^3}.$$

The sign of $\frac{\partial^2 v(k+1)}{\partial m^2}$ in the range $h \in [10000 \ 30000] \ ft$ of altitudes of interest is always negative for $v(k)$ greater than 55 m/s, which is an unrealistically low airspeed in the leg of flight considered in our case study. Therefore we conclude that the mass that maximizes $v(k+1)$ under the constraint $m \in [\underline{m}(k^-) \quad \overline{m}(k^-)]$ is either $m^{max}(k)$ given by (11), if $m^{max}(k)$ belongs to $[\underline{m}(k^-) \quad \overline{m}(k^-)]$ or one of the extremes of $[\underline{m}(k^-) \quad \overline{m}(k^-)]$. In addition, we can also conclude that the minimum value of $v(k+1)$ is attained at one of the extremes of $[\underline{m}(k^-) \quad \overline{m}(k^-)]$.

REFERENCES

[1] Paglione, M., Garcia-Avello, C., Vivona, R., Green, S., *A collaborative approach to trajectory modeling and validation*, Digital Avionics Systems Conference, USA, 2005.

[2] Chang, E., Hu, R., Lai, D., Li, R., Scott, Q., Tyan, T., *The story of Mode S*, Final Report, available on line at the URL http://mit.edu/6.933/www/Fall2000/mode-s/mode-s.pdf.

[3] RTCA *Minimum aviation system performance standards for the automatic surveillance-broadcast (ADS-B)*, DO-242A, January, 1998.

[4] Innocenti, M., Gelosi, P, Pollini, L., *Air traffic management using probability function fields*, AIAA Guidance, Navigation, and Control Conference and Exhibit, 1999.

[5] Frazzoli, E., Mao, Z.-H., Oh, J.-H., Feron, E., *Resolution of Conflicts Involving Many Aircraft via Semidefinite Programming*, Journal of Guidance, Control, and Dynamics, Vol. 24, Issue 1, 2001.

[6] Paielli, R.A., *Modelling Maneuver Dynamics in Air Traffic Control Conflict Resolution*, Journal of Guidance, Control, and Dynamics, Vol. 26, Issue 3, 2003.

[7] Mao, Z.-H., Dugail, D., Feron, E., Bilimoria, K., *Stability of Intersecting Aircraft Flows Using Heading-Change Maneuvers for Conflict Avoidance*, IEEE Transactions on Intelligent Transportation Systems, Vol. 6, Issue 4, 2005.

[8] Paielli, R.A., Erzberger, H., *Conflict Probability Estimation for Free Flight*, Journal of Guidance, Control, and Dynamics, Vol. 20, Issue 3, 1997.

[9] Paielli, R.A., H. Erzberger, H., *Conflict Probability Estimation Generalized to Non-Level Flight*, Air Traffic Control Quarterly, Vol. 7, Issue 3, 1999.

[10] Yang, L.C., Kuchar, J.K., *Prototype Conflict Alerting System for Free Flight*, Journal of Guidance, Control, and Dynamics, Vol. 20, Issue 4, 1997.

[11] Yang, L., Yang, J.H., Kuchar, J., Feron, E. *A Real-Time Monte Carlo Implementation for Computing Probability of Conflict*, AIAA Guidance, Navigation, and Control Conference and Exhibit, 2004.

[12] Chaloulos, G., Lygeros, J., *Effect of wind correlation on aircraft conflict probability*, Journal of Guidance, Control and Dynamics, Vol. 30, Issue 6, 2007.

[13] Blom, H.A.P., Krystul, G.J., Bakker, G.J., Klompstra, M.B., Obbink, B.K., Free flight collision risk estimation by sequential Monte Carlo simulation, In *Stochastic Hybrid Systems*, C.G. Cassandras and J. Lygeros (eds.), CRC/Taylor & Francis, 2007. Available online at the URL http://www.nlr.nl/id 7791/l en.pdf

[14] Tomlin, C., Mitchell, I., Ghosh, R., *Safety verification of conflict resolution manoeuvres*, IEEE Transactions on Intelligent Transportation Systems, Vol. 2, Issue 2, 2001.

[15] McConkey, E.D., Bolz, E.H., *Analysis of the vertical accuracy of the CTAS trajectory prediction process*, Report from Science Applications International Corporation for NASA Ames Research Center, Moffett Field, California, 2002. Available online at the URL http://as.nasa.gov/aatt/rto/RTOFinal68_1.pdf.

[16] Mueller, K.T., Bortins, R., Schleicher, D.R., Sweet, D., *Effect of uncertainty on en route descent advisor (EDA) predictions*, AIAA 4^{th} Aviation Technology, Integration and Operations (ATIO) Forum, Chicago, Illinois, 2004.

[17] EUROCONTROL Experimental Center, *User manual for the base of aircraft data (BADA)*, Version 3.6, 2004. Available online at the URL http://www.eurocontrol.int/eec/public/standard_page /proj_BADA.html

[18] Gordon, N.J., Salmond, D.J., Smith, A.F.M., *Novel approach to nonlinear/non-Gaussian Bayesian state estimation*, IEE Proc. F, vol. 140, no. 2, 1993.

[19] Van der Merwe, R., Doucet, A., de Freitas, J.F.G., Wan E., *The unscented particle filter*, Advances in Neural Information Processing Systems, 13, 2000.

[20] Doucet, A., de Freitas, N., Gordon, N. (editors), *Sequential Monte Carlo Methods in Practice*, Springer-Verlag, 2001.

[21] Arulampalam, M.S., Maskell, S., Gordon, N., Clapp, T., *A tutorial on particle filters for online nonlinear/non-Gaussian Bayesian tracking*, IEEE Transactions on Signal Processing, Vol. 50, Issue 2, 2002.

[22] Künsch, H.R., *Recursive Monte Carlo filters: algorithms and theoretical analysis*, The Annals of Statistics, vol. 33, no. 5, 2005.

[23] Schweppe, F.C., *Recursive state estimation: unknown but bounded errors and system inputs*, IEEE Transactions on Automatic Control, vol. 13, no. 1, 1968.

[24] Bertsekas, D.P., Rhodes, I.B., *Recursive state estimation for a set-membership description of uncertainty*, IEEE Transactions on Automatic Control, Vol. 16, Issue 2, 1971.

[25] Chisci, L., Garulli, A., Zappa, G., *Recursive state bounding by parallelotopes*, Automatica, Vol. 32, Issue 7, 1996.

[26] Polyak, B.T., Nazin, S.A., Durieu, C., Walter, E., *Ellipsoidal parameter or state estimation under model uncertainty*, Automatica, Vol. 40, Issue 7, 2004.

[27] Balestrino, A., Caiti, A., Crisostomi, E., *Particle filtering within a set-membership approach to state estimation*, IEEE Mediterranean Conference on Control and Automation, Ancona, Italy, 2006.

[28] Balestrino, A., Caiti, A., Crisostomi, E., *PP algorithm for particle filtering within ellipsoidal regions*, Nonlinear Statistical Signal Processing Workshop, Cambridge, 2006.

[29] Bai, E.-W., Ye, Y., Tempo, R., *Bounded error parameter estimation: a sequential analytic center approach*, IEEE Transactions on Automatic Control, Vol 44, Issue 6, June 1999.

[30] Lecchini-Visintini, A., Glover, W., Lygeros, J., Maciejowski, J. *Monte Carlo Optimisation for Conflict Resolution in Air Traffic Control*, IEEE Transactions on Intelligent Transportation Systems, Vol. 7, Issue 4, 2006.

[31] FAA, *Radar Vectoring*, Pilot/Controller Glossary, 2008. Available online at the URL http://www.caa.gov.tw/en/files/2008PCG.pdf.

[32] FAA/EUROCONTROL Action Plan 16, White Paper on *Common Trajectory Prediction related terminology*, RDCOM-AP16 Core Team, 2004.

[33] Vilaplana, M.A., Gallo, E., Navarro, F.A., *Towards a formal language for the common description of aircraft intent*, Digital Avionics Systems Conference, 2005.

[34] Mondoloni, S., Ballin, M.G., Palmer, M.T., *Airborne conflict resolution for flow-restricted transition airspace*, AIAA Avation Technology, Integration and Operations (ATIO) Technical Forum

[35] Mondoloni, S., Ballin, M.G., *Evaluation of an airborne resolution algorithm for flow-restricted transition airspace*, AIAA Guidance, Navigation and Control Conference and Exhibit, 2004.

[36] Cole, R.E., Richard, C., Kim, S., Bailey, D., *An assessment of the 60 km rapid update cycle (RUC) with near real-time aircraft reports*, Technical Report NASA/A-1, MIT Lincoln Laboratory, July 15, 1998.

[37] Schwartz, B.E., Benjamin, S.G., Green, S.M., Jardin, M.R., *Accuracy of RUC-1 and RUC-2 wind and aircraft trajectory forecasts by comparison with ACARS observations*, Weather and Forecasting, vol. 15, Issue 3, 2000.

[38] Kitsios, I., Lygeros, J., *Final glide-back envelope computation for reusable launch vehicle using reachability*, IEEE Conference on Decision and Control, Seville, Spain, 2005.

[39] MacKay, D.J.C., *Information theory, inference, and learning algorithms*, Cambridge University Press, 2007.

[40] Lee, D.S., Chia, N.K.K., *A particle algorithm for sequential bayesian parameter estimation and model selection*, IEEE Transactions on Signal Process., Vol. 50, No. 2, February 2002.

[41] Andrieu, C., Doucet, A., *Recursive Monte Carlo algorithms for parameter estimation in general state space models*, IEEE Workshop Statist. Signal Process., Singapore, August 2001.

[42] Lang, L., Chen, W.-S., Bakshi, B.R., Goel, P.K., Ungarala, S., *Bayesian estimation via sequential Monte Carlo sampling - Constrained dynamic systems*, Automatica, Vol. 43, Issue 9, 2007.